

Cross section of ultrahigh-energy neutrinos: Estimation of the uncertainties due to parton distribution functions

M. E. Mosquera^{1,2,*} and O. Civitarese^{2,†}

¹Facultad de Ciencias Astronómicas y Geofísicas, Universidad Nacional de La Plata, Paseo del Bosque S/N (1900) La Plata, Argentina

²Departamento de Física, Universidad Nacional de La Plata, C.C. 67 (1900) La Plata, Argentina



(Received 22 May 2020; accepted 7 August 2020; published 25 August 2020)

In this work we analyze the effect of uncertainties in parton distribution functions upon the calculation of cross sections for ultrahigh-energy neutrinos. As a detector we choose ^{12}C . The elementary diagrams for the neutrino-proton and neutron interactions have been calculated at quark level using nuclear parton distribution functions and their corresponding error bars, as given by the Jyvaskyla group. The leptonic sector of the current-current interactions includes active-sterile neutrino mixing. From the calculated cross section we have set limits on the values of the mixing parameters.

DOI: [10.1103/PhysRevC.102.025803](https://doi.org/10.1103/PhysRevC.102.025803)

I. INTRODUCTION

The physics of neutrino oscillations and its matter effect are well understood [1,2]. The value of the elements of the mixing matrix, amplitudes, and square mass differences for three active-flavor neutrinos have been determined experimentally [3,4], with the exception of the absolute neutrino mass scale. Results published by LSND (Liquid Scintillator Neutrino Detector) and MiniBoone (Mini Booster Neutrino Experiment) have established limits for the existence of at least one extra sterile neutrino (ν_s) [5,6]. The detection of high energy neutrinos is a crucial step in the search of new physics beyond the standard model of electroweak interactions [7]. Recently, the IceCube Neutrino Observatory determined the extragalactic origin of few ultrahigh-energy neutrinos, with energies in the range of GeV to EeV, giving information about the deep inelastic scattering of neutrinos by nucleons [8]. These findings may help in understanding both the structure of the incoming neutrinos as well as that of the hadrons (nucleons) of the target.

In this work we are reporting on calculations of the neutrino-nucleon cross section, for IceCube energies, starting from the elementary neutrino-quark interactions, for both neutral and charged currents [9–12]. We have taken the CT14NLO parton distribution function (PDF) as the free-proton baseline [13–15] and included the corrections to these functions reported in Ref. [16] by the Jyvaskyla group. As a first step we considered a single type of neutrino and then turned on the mixing between active and sterile neutrinos in the leptonic sector. The theoretical results are compared with the available data [8].

This work is organized as follows. In Sec. II we present the formalism needed to compute the neutrino-nucleon cross

section. In Sec. III we show and discuss the results of our calculations. The conclusions are drawn in Sec. IV.

II. FORMALISM

Neutrinos and antineutrinos interact with nucleons through neutral and charged currents,

$$\begin{aligned} \nu_l + N &\rightarrow \nu_l + N, \\ \nu_l + N &\rightarrow l + X, \end{aligned} \quad (1)$$

where N and X are nucleons and l is a charged lepton. To compute the cross sections of the previous reactions, we follow the procedure developed in Ref. [12]. In order to include active-sterile neutrino oscillations, we have expressed the neutrino of flavour δ as a combination of the mass eigenstates [17], that is

$$|\nu_\delta\rangle = \sum_a U_{\delta a} |\nu_a\rangle, \quad (2)$$

where U_{ij} is the unitary mixing matrix. The mass of the eigenstate $|\nu_a\rangle$ is m_a , and the mass for the flavor neutrino $|\nu_\delta\rangle$ is given by $\langle m_\delta \rangle = \sum_a |U_{\delta a}|^2 m_a$ (ignoring CP phases), therefore $p_0^2 = |\vec{p}|^2 + m_\delta^2$.

A. Charged current process

The currents are defined, for both the leptonic and hadronic sectors, as

$$(J_{\text{lep}})_\mu = \bar{u}_{\nu_\delta}(p, s_p) \gamma_\mu (1 - \gamma_5) u_l(q, s_q), \quad (3)$$

$$(J_{\text{had}})_\mu = \bar{u}_N(k, s_k) \gamma_\mu (1 - \gamma_5) u_X(z, s_z), \quad (4)$$

where p (s_p) and k (s_k) are the four-momenta (spins) of the incident neutrino of flavor δ and the nucleon N , respectively, and q (s_q) and z (s_z) are the four-momenta (spins) of the charged lepton and of the nucleon X . The symbol u_y stands for the Dirac spinor of the particle y . After some algebra and the use of the Mandelstam variables [$s = (p + k)^2$,

*mmosquera@fcaglp.unlp.edu.ar

†osvaldo.civitarese@fisica.unlp.edu.ar

$t = -Q^2 = (p - q)^2$, $u = (q - k)^2$] and the Bjorken scaling variables x and y [7,18],

$$x = \frac{-Q^2}{2k \cdot (p - q)}, \quad (5)$$

$$y = \frac{k \cdot (p - q)}{k \cdot p}, \quad (6)$$

the charged current neutrino-quark cross section, in the laboratory frame, is written as

$$\frac{d\sigma_{\nu q}}{dx dy} = xs \frac{g^2}{\pi} \frac{1}{\left(1 - \frac{m_N^2 + m_\delta^2}{s}\right)^2 - \frac{2m_N m_\delta}{s^2}} \frac{1 - (m_N^2 + m_l^2)s^{-1}}{\left[xy(s - m_N^2 - m_\delta^2) + M_W^2\right]^2} \sum_{a,b} U_{\delta b}^\dagger U_{\delta a} \left[1 + O\left(\frac{m_N^2}{s}\right) + O\left(\frac{m_\delta^2}{s}\right)\right] \quad (7)$$

where M_W is the mass of the W-boson, m_N is the nucleon mass and m_l is the mass of the charged lepton, m_δ is the average neutrino mass and g is the coupling constant ($g = M_W^2 G_F$). See Ref. [12] for details.

Similarly the cross section for the charged process with anti-quarks is written as

$$\frac{d\sigma_{\nu \bar{q}}}{dx dy} = xs \frac{g^2}{\pi} \frac{1}{\left(1 - \frac{m_N^2 + m_\delta^2}{s}\right)^2 - \frac{2m_N m_\delta}{s^2}} \frac{1 - (m_N^2 + m_l^2)u^{-1}}{\left[xy(s - m_N^2 - m_\delta^2) + M_W^2\right]^2} \frac{u^2}{s^2} \sum_{a,b} U_{\delta b}^\dagger U_{\delta a} \left[1 + O\left(\frac{m_N^2}{u}\right) + O\left(\frac{m_\delta^2}{u}\right)\right].$$

Since the nucleon is composed of valence quarks and a sea of quark-antiquark pairs [19], the cross section can be written as

$$\frac{d\sigma}{dx dy} = \frac{d\sigma_{\nu q}}{dx dy} f_d(x, Q^2) + \frac{d\sigma_{\nu \bar{q}}}{dx dy} f_{\bar{u}}(x, Q^2),$$

where $f_i(x, Q^2)$ are the parton distribution functions of quarks [7,18,20]:

$$\begin{aligned} f_d(x, Q^2) &= \frac{u_v(x, Q^2) + d_v(x, Q^2)}{2} + s_s(x, Q^2) + \frac{u_s(x, Q^2) + d_s(x, Q^2)}{2} + b_s(x, Q^2), \\ f_u(x, Q^2) &= \frac{u_v(x, Q^2) + d_v(x, Q^2)}{2} + c_s(x, Q^2) + \frac{u_s(x, Q^2) + d_s(x, Q^2)}{2} + t_s(x, Q^2), \\ f_{\bar{d}}(x, Q^2) &= \frac{u_s(x, Q^2) + d_s(x, Q^2)}{2} + s_s(x, Q^2) + b_s(x, Q^2), \\ f_{\bar{u}}(x, Q^2) &= \frac{u_s(x, Q^2) + d_s(x, Q^2)}{2} + c_s(x, Q^2) + t_s(x, Q^2). \end{aligned} \quad (8)$$

The subscripts v and s denote valence and sea contributions of each quark flavor (u, d, s, b, c , and t) to the proton [21].

B. Neutral current process

The currents for the scattering are

$$(J_{\text{lep}})_\mu = \bar{u}_{\nu_\delta}(p, s_p) \gamma_\mu (1 - \gamma_5) u_{\nu_\delta}(q, s_q), \quad (9)$$

$$(J_{\text{had}})_\mu = \bar{u}_N(k, s_k) \gamma_\nu (g_A - g_V \gamma_5) u_N(z, s_z), \quad (10)$$

where p (s_p) and k (s_k) are the four-momenta (spins) of incident neutrino of flavor δ and of the nucleon respectively, q (s_q) and z (s_z) are the four-momenta (spins) of the outgoing particles, and g_A and g_V are axial and vector couplings [20]. In terms of Bjorken scaling variables, we write

$$\begin{aligned} \frac{d\sigma_{\nu q}}{dx dy} &= xs \frac{g^2}{4\pi} \frac{1}{\left(1 - \frac{m_N^2 + m_\delta^2}{s}\right)^2 - \frac{2m_N m_\delta}{s^2}} \frac{1}{\left[xy(s - m_N^2 - m_\delta^2) + M_Z^2\right]^2} \\ &\times \sum_{a,b} C_{abcd} \left\{ (g_A - g_V)^2 \frac{u^2}{s^2} [1 + \mathcal{W}] + (g_A + g_V)^2 [1 + \mathcal{R}] + (g_V^2 - g_A^2) \frac{m_N^2 t}{s^2} [1 + \mathcal{S}] \right\}, \end{aligned} \quad (11)$$

where the functions \mathcal{W} , \mathcal{R} , and \mathcal{S} are $O\left(\frac{m_N^2}{u}\right) + O\left(\frac{m_\delta^2}{u}\right)$, $O\left(\frac{m_N^2}{s}\right) + O\left(\frac{m_\delta^2}{s}\right)$, and $O\left(\frac{m_\delta^2}{t}\right)$, respectively, and M_Z is the mass of the Z boson. See Ref. [12] for more details.

Proceeding similarly, the cross section for the neutral neutrino-antiquark channel is written as

$$\frac{d\sigma_{\nu\bar{q}}}{dx dy} = x s \frac{g^2}{4\pi} \frac{1}{\left(1 - \frac{m_N^2 + m_\delta^2}{s}\right)^2 - \frac{2m_N m_\delta}{s^2} [xy(s - m_N^2 - m_\delta^2) + M_Z^2]^2} \frac{1}{\left(1 - \frac{m_N^2 + m_\delta^2}{s}\right)^2 - \frac{2m_N m_\delta}{s^2} [xy(s - m_N^2 - m_\delta^2) + M_Z^2]^2} \\ \times \sum_{a,b} \mathcal{C}_{abcd} \left\{ (g_A + g_V)^2 \frac{u^2}{s^2} [1 + \mathcal{W}] + (g_A - g_V)^2 [1 + \mathcal{R}] + (g_V^2 - g_A^2)^2 \frac{m_N^2 t}{s^2} [1 + \mathcal{S}] \right\}.$$

Introducing the quark-parton model, the cross section takes the form

$$\frac{d\sigma}{dx dy} = \sum_{q=u,d} \frac{d\sigma_{\nu q}}{dx dy} f_q(x, Q^2) + \sum_{q=u,d} \frac{d\sigma_{\nu\bar{q}}}{dx dy} f_{\bar{q}}(x, Q^2),$$

where $f_i(x, Q^2)$ stands for the parton distribution functions of quarks.

C. Parton distribution functions (PDFs) and their uncertainties

The bound-proton parton distribution functions (PDFs) are defined relative to the free-proton PDF by a factor $R_\alpha^A(x, Q^2)$ as explained in Ref. [16]:

$$\alpha_i^A(x, Q^2) = R_\alpha^A(x, Q^2) \alpha_i(x, Q^2), \quad (12)$$

where the factor R_i^A is the nuclear modification factor and α stands for the quark. The free-proton baseline used in this work is CT14NLO [13–15] and the uncertainties in the PDF are the ones published by the Jyvaskyla Group [16]. We have used the central value and the total uncertainties for the R_α^A

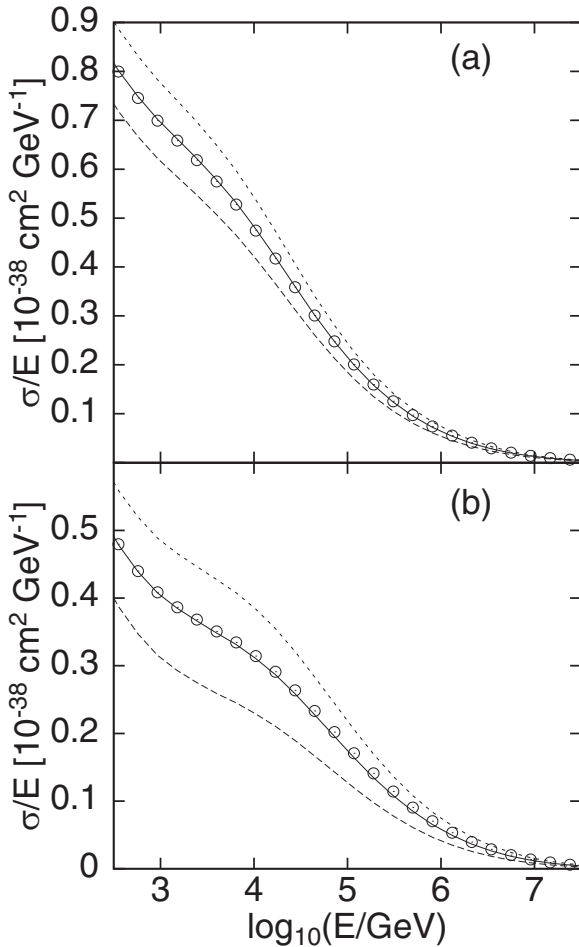


FIG. 1. Neutrino cross section for charged currents, as a function of the neutrino energy. (a) neutrinos; (b) antineutrinos. Solid line: central value of R_α^A ; long-dashed line: lower value for R_α^A ; small-dashed line: higher value of R_α^A [16]; circle: CT14NLO PDF [13–15].

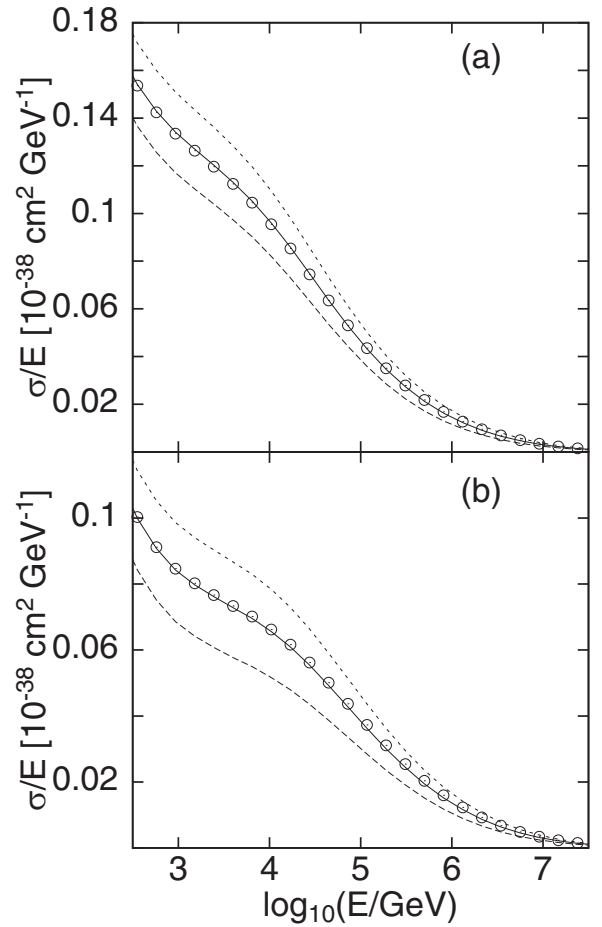


FIG. 2. Neutrino cross section for neutral current (mediated by a Z boson) as a function of the neutrino energy. (a) neutrinos; (b) antineutrinos. Solid line: central value of R_α^A ; long-dashed line: lower value for R_α^A ; small-dashed line: higher value of R_α^A [16]; circle: CT14NLO PDF [13–15].

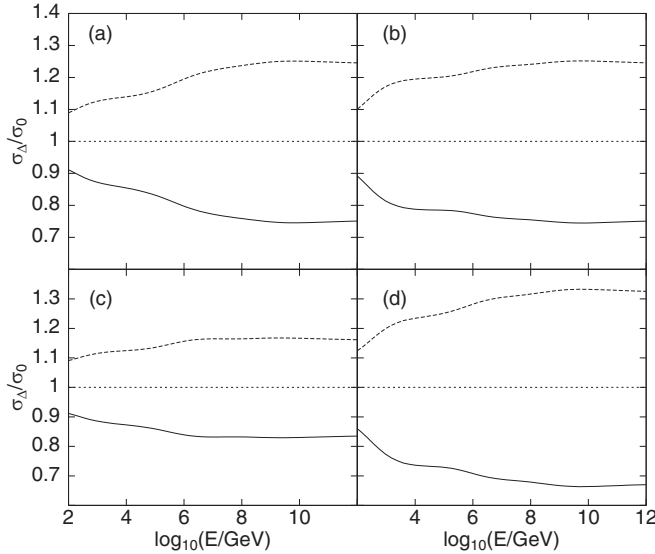


FIG. 3. Ratio of the neutrino cross section computed with and without errors, as a function of the neutrino energy. Top row: neutral current [(a) and (b)]; bottom row: charged current [(c) and (d)]. Left column: neutrinos [(a) and (c)]; right column: antineutrinos [(b) and (d)]. Solid line: lower value for R_α^A ; dashed line: higher value of R_α^A .

factor (see Fig. 9 of Ref. [16]) for ^{12}C (target). We have assumed that the factor R_α^A does not strongly depend on the Bjorken variable y . We have taken the values of R_α^A for $Q^2 = 1.69 \text{ GeV}^2$, since the nuclear modification factor is larger for smaller values of Q^2 . Using this nuclear modification factor we have recalculated the parton distribution functions and the cross sections as function of the neutrino energy.

III. RESULTS

We have performed two different analyses to study the neutrino-nucleus cross section. First we included the uncertainties in the PDF, and then we also considered the effects associated with the active-sterile neutrino mixing.

A. Effects of the error bars of the parton functions [16]

As a first step we have analyzed the contribution of the factor R_α^A for each one of the quarks. We have found that the quark d is responsible for the larger modification to the neutrino cross section (both charged and neutral current) and to the antineutrino cross section.

The results corresponding to the uncertainties of the PDF for all quarks are shown in Figs. 1 and 2. As said before, the value of the nuclear modification factor, for $Q^2 = 1.69 \text{ GeV}^2$, was taken from Ref. [16].

Figure 3 shows the ratio between the modified cross section (σ_Δ) and the standard neutrino cross section obtained with the central values of the PDF (σ_0). As one can see, the ratio becomes larger for larger values of the neutrino energy. In the range of energies $4 < \log_{10}(E/\text{GeV}) < 7$ the changes in the calculated cross sections due to the uncertainties of the PDF vary between 10% and 30%.

TABLE I. Best fit of the active-sterile neutrino mixing angle.

R_α^A	$\cos \theta_{14} \pm \sigma$	χ_{\min}^2
Higher value (R_H)	$0.61^{+0.15}_{-0.18}$	1.63
Central value (R_C)	$0.71^{+0.19}_{-0.18}$	1.58
Lower value (R_L)	$0.85^{+0.15}_{-0.17}$	1.53

B. Constrains on the active-sterile mixing angle

The active-sterile neutrino mixing matrix is written as

$$U = \begin{pmatrix} c_{13}c_{12} & c_{13}s_{12} & s_{13}e^{-i\phi} & 0 \\ a_1 & b_1 & c_{13}s_{23} & 0 \\ a_2 & b_2 & c_{13}c_{23} & 0 \\ 0 & 0 & 0 & 1 \end{pmatrix} \begin{pmatrix} c_{14} & 0 & 0 & s_{14} \\ 0 & 1 & 0 & 0 \\ 0 & 0 & 1 & 0 \\ -s_{14} & 0 & 0 & c_{14} \end{pmatrix}$$

with the usual notation: $c_{ij} = \cos \theta_{ij}$ and $s_{ij} = \sin \theta_{ij}$; and $a_1 = -c_{23}s_{12} - s_{23}c_{12}s_{13}e^{i\phi}$, $b_1 = c_{23}c_{12} - s_{23}s_{12}s_{13}e^{i\phi}$, $a_2 = s_{23}s_{12} - c_{23}c_{12}s_{13}e^{i\phi}$, $b_2 = -s_{23}c_{12} - c_{23}s_{12}s_{13}e^{i\phi}$. The values for the active neutrino oscillation parameters were extracted from Ref. [22]. We have considered the active-sterile neutrino mixing angle as a free parameter and fixed the mass squared difference between the active and sterile states [12]. The values for g_A and g_V were taken from [20].

We performed a χ^2 test in order to find the best value for θ_{14} . To perform this analysis we calculated the electron-type neutrino and antineutrino cross sections for charged and neutral channels and for different values of the mixing angles. The theoretical results, obtained with the higher, lower, and central values of the parameters R_α^A [16], and the available

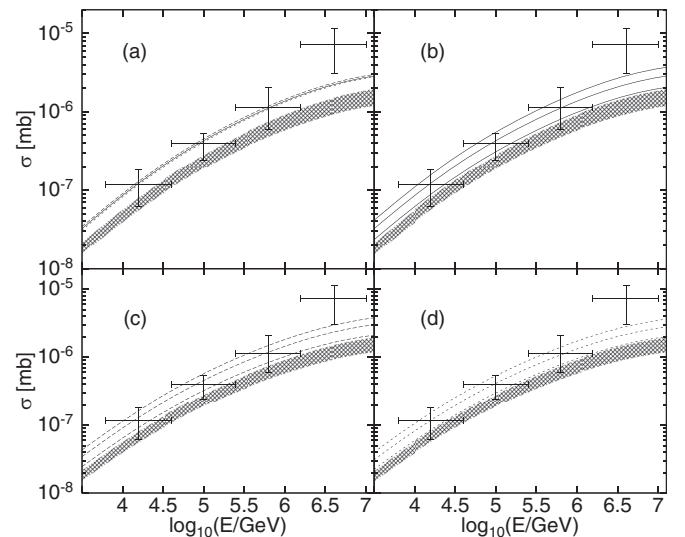


FIG. 4. Total neutrino scattering cross section (charged and neutral current channels) for neutrinos and antineutrinos, as a function of the neutrino energy. (a) Best fit of θ_{14} for each value of R_α^A . (b) Best fit obtained using (R_C). (c) Best fit obtained using (R_L). (d) Best fit obtained using (R_H). Large crosses: available data with experimental error bars [8]; shaded band: standard cross section using the theoretical errors of Ref. [16]; lines: cross section with active-sterile neutrino oscillations at the best fit of θ_{14} and at one standard deviation.

IceCube data [8] were taken as the input of the minimization. Table I shows the best fit for the active-sterile mixing angle θ_{14} , for each of the limits for the PDF.

In Fig. 4 we present the data, the standard cross section with the inclusion of the PDF with theoretical error bars of Ref. [16] (dark band of the figure), and the cross section with the active-sterile mixing at the best value of the mixing angle and at one standard deviation.

IV. CONCLUSIONS

In this work we have included the uncertainties of the parton distribution function reported in Ref. [16] by the Jyväskylä Group in the computation of the neutrino-nucleon cross section at high energies, both for charged and neutral current processes. We have found that the cross section is modified by the inclusion of the PDF uncertainties, and the

percentage of change depends on the neutrino energy: the larger the neutrino energy, the larger the change in the cross section. The larger variation in σ is of the order of 30%.

From these calculations we were able to set constraints on the active-sterile mixing angle by the comparison of the theoretical results with the experimental data of IceCube. The results for the different cases (lower, central, and higher values of R_α^A) overlap at $\cos \theta_{14} \approx 0.75$, a value which is consistent with our previous results [12].

ACKNOWLEDGMENTS

This work was supported by the grant PIP-616 of the National Research Council of Argentina (CONICET), and by a research grant of the National Agency for the Promotion of Science and Technology (ANPCYT) of Argentina.

-
- [1] S. Bilenyk, [arXiv:1907.01472](#).
 - [2] A. Y. Smirnov, *Phys. Scr.* **T121**, 57 (2005).
 - [3] A. B. McDonald, *Int. J. Mod. Phys. A* **31**, 1630048 (2016).
 - [4] S. Fukuda *et al.*, *Nucl. Instrum. Methods Phys. Res. A* **501**, 418 (2003).
 - [5] A. A. Aguilar-Arevalo *et al.* (MiniBooNE Collaboration), *Phys. Rev. Lett.* **121**, 221801 (2018).
 - [6] C. Athanassopoulos *et al.* (LSND Collaboration), *Phys. Rev. Lett.* **77**, 3082 (1996).
 - [7] R. N. Mohapatra and P. B. Pal, *Massive Neutrinos in Physics and Astrophysics*, 3rd ed., World Scientific Lecture Notes in Physics Vol. 72 (World Scientific, Singapore, 2004).
 - [8] Y. Xu and (IceCube Collaboration), in XXVI International Workshop on Deep-Inelastic Scattering and Related Subjects, 16–20 April 2018, Kobe [PoS **DIS2018**, 19 (2018)].
 - [9] A. Connolly, R. S. Thorne, and D. Waters, *Phys. Rev. D* **83**, 113009 (2011).
 - [10] A. Cooper-Sarkar, P. Mertsch, and S. Sarkar, *J. High Energy Phys.* **08** (2011) 042.
 - [11] M. M. Block, L. Durand, and P. Ha, *Phys. Rev. D* **89**, 094027 (2014).
 - [12] B. E. Melendez, M. E. Mosquera, and O. Civitarese, *Phys. Rev. C* **101**, 035806 (2020).
 - [13] S. Dulat *et al.*, *Phys. Rev. D* **93**, 033006 (2016).
 - [14] H. L. Lai, M. Guzzi, J. Huston, Z. Li, P. M. Nadolsky, J. Pumplin, and C. P. Yuan, *Phys. Rev. D* **82**, 074024 (2010).
 - [15] J. Gao *et al.*, *Phys. Rev. D* **89**, 033009 (2014).
 - [16] K. J. Eskola, P. Paakkinen, H. Paukkunen, and C. A. Delgado, *Eur. Phys. J. C* **77**, 163 (2017).
 - [17] T. Faestermann, F. Bosch, R. Hertenberger, L. Maier, R. Krücken, and G. Rugel, *Phys. Lett. B* **672**, 227 (2009).
 - [18] R. Gandhi *et al.*, *Astropart. Phys.* **5**, 81 (1996).
 - [19] R. P. Feynman, *Phys. Rev. Lett.* **23**, 1415 (1969).
 - [20] C. Giunti and C. W. Kim, *Fundamentals of Neutrino Physics and Astrophysics* (Oxford University Press, Oxford, 2007).
 - [21] R. Gandhi, *Nucl. Phys. B Proc. Suppl.* **91**, 453 (2001).
 - [22] M. Tanabashi *et al.* (Particle Data Group), *Phys. Rev. D* **98**, 030001 (2018).